THE ROLE OF ESTER SULFATE AND ORGANIC DISULFIDE IN MERCURY METHYLATION IN PEATLAND SOILS

Caroline E. Pierce [a], Olha S. Furman [ab], Sarah L. Nicholas [ac], Jill Coleman Wasik [d], Caitlin M. Gionfriddo [ef], Ann M. Wymore [e], Stephen D. Sebestyen [g], Randall K. Kolka [g], Carl P.J. Mitchell [h], Natalie A. Griffiths [i], Dwayne A. Elias [e], Edward A. Nater [a], and Brandy M. Toner [a]*

[a] Department of Soil, Water, and Climate, University of Minnesota, St. Paul, MN 55108 USA

[b] Current affiliation: Department of Agriculture, Water, and the Environment, Australian Government, Canberra, Australia

[c] Current affiliation: Brookhaven National Laboratory - National Synchrotron Light Source II, Upton, NY 11973 USA

[d] Plant and Earth Science Department, University of Wisconsin River Falls, River Falls, WI 54022 USA

[e] Biosciences Division, Oak Ridge National Laboratory, Oak Ridge, TN, 37831 USA

[f] Current affiliation: Smithsonian Environmental Research Center, Edgewater, MD 21037 USA

[g] USDA Forest Service, Northern Research Station, Grand Rapids, MN 55744 USA

[h] Department of Physical and Environmental Sciences, University of Toronto Scarborough, Scarborough, ON Canada

[i] Environmental Sciences Division, Oak Ridge National Laboratory, Oak Ridge, TN 37831 USA

23   SYNOPSIS

24   Organic sulfur species in peat are important reactants (ester sulfate) and products (organic

25   disulfide) in mercury methylation. Organic sulfur species also have the potential to limit the

26   bioavailability of mercury for methylation (organic monosulfides).

27

28   *Corresponding author email: toner@umn.edu

29

ABSTRACT

We examined the composition and spatial correlation of sulfur and mercury pools in peatland soil profiles by measuring sulfur 1s X-ray absorption near-edge structure (XANES) and mercury concentrations by cold vapor atomic fluorescence spectroscopy. Also investigated were the methylation/demethylation rate constants and the presence of *hgc*AB genes with depth. Methylmercury (MeHg) concentration and organic disulfide were spatially correlated and had a significant positive correlation ($p < 0.05$). This finding is consistent with these species being products of dissimilatory sulfate reduction. Conversely, a significant negative correlation between organic monosulfides and MeHg was observed, which is consistent with a reduction in Hg(II) bioavailability via complexation reactions. Finally, a significant positive correlation between ester sulfate and instantaneous methylation rate constants was observed, which is consistent with ester sulfate being a substrate for mercury methylation via dissimilatory sulfate reduction. Our findings point to the importance of organic sulfur species in mercury methylation processes, as substrates and products, as well as potential inhibitors of Hg(II) bioavailability. For a peatland system with sub-μmol L^{-1} porewater concentrations of sulfate and hydrogen sulfide, our findings indicate that the solid-phase sulfur pools, which have a much larger sulfur concentration range, may be accessible to microbial activity or exchanging with the porewater.
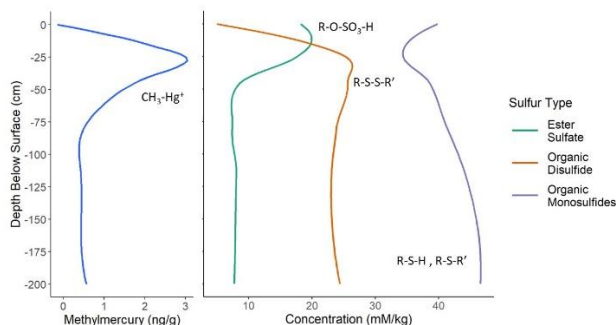
61 **Abstract Art**

63

65

1. INTRODUCTION

67   Globally, boreal peatlands cover a land area of 4 million km^2, primarily in Russia, Canada, and the

68   USA [1]. Within Minnesota, boreal peatlands cover a land area of 24,000 km^2 [2]. Boreal peatlands

69   are hot spots for the production of methylmercury (MeHg) that lead to toxic and environmentally

70   detrimental levels [3–5]. Methylmercury released from peatlands to aquatic systems can be

71   biomagnified in the food web to top predatory fish that humans and wildlife consume [6]. While

72   sulfate-reducing bacteria (SRB) are considered to be important producers of MeHg not all SRB

73   methylate mercury [7]. Cause and effect studies in peatlands demonstrate that enhanced availability

74   of sulfate leads to increased MeHg concentrations but the detailed information of how sulfur is

75   transformed in organic soils remains unknown [8,9]. Methanogens and some iron-reducing bacteria

76   (IRB) also produce MeHg within boreal peatlands [10–12]. However, the role of methanogens and

77   IRB in mercury methylation is outside the scope of this article. We explore the interactions of

78   sulfur and mercury via microbial sulfate reduction within a boreal peatland. It is unknown why

79 microbes methylate mercury though there are hypotheses such as detoxification of the cell, carbon

80 metabolism, and metal homeostasis [13,14].

81

82 Biogeochemically linked elements, sulfur and mercury, enter ombrotrophic bogs (see section 2.1)

83 through atmospheric deposition and are cycled in the soil profile by physical, chemical, and

84 biological processes. Cycling is especially active at depths where distinct contrasts in physical and

85 chemical properties, such as water content and oxidation-reduction conditions occur [15–18]. As an

86 example of a chemical process, mercury has a high binding affinity for reduced organic sulfur

87 (e.g., thiols) [19–21]. As an example of a biological process, dissimilatory SRB populations catalyze

88 the reduction of sulfur and mercury methylation in peatland soils [8,9,22,23]. Although porewater

89 sulfate pools are small, oxidation reactions during periods of lowered water tables may recycle

90 oxidized organic sulfur that can sustain sulfate reduction rates and net MeHg production following

91 wetting events [17,24,25]. Studies in low-sulfate environments demonstrate that organic sulfur

92 compounds can be an important component of dissimilatory sulfate reduction [26]. Genomic studies

93 have shown that some SRB are capable of utilizing ester sulfate [27]. However, this pathway has not

94 been co-demonstrated in SRB that also methylate mercury. The functional genes that encode for

95 mercury methylation in anaerobic microorganisms have been identified as *hgc*AB [10,28]. We are not

96 aware of literature about the depth distribution of *hgc*AB genes within boreal peat.

97

98 In this study we measured the abundance and speciation of mercury and sulfur, rates of methylation

99 and demethylation, and the presence of *hgc*AB genes in peat profiles. Most lab and field studies

100 to date have focused on inorganic sulfate as a driver for mercury methylation [8,18,21,29] but bogs have

101 little inorganic sulfur [30,31]. Our objective was to investigate the role of organic sulfur species, as

102 opposed to inorganic sulfur species, in peatland soil as important reactants and products in mercury

103 methylation. In a climate with an increasingly variable water table (i.e., longer drought with deeper

104 water table position) a greater volume of peat may be exposed to biogeochemical processes that

105 are able to generate ester sulfate and MeHg [15,32–37].

106

2.   MATERIALS AND METHODS

2.1 Site Description

109 The field site, the S1 bog, is an ombrotrophic bog with a black spruce (*Picea mariana*) and

110 tamarack (*Larix laricina*) overstory, located at the United States Department of Agriculture

111 (USDA) Forest Service Marcell Experimental Forest (MEF) in northern Minnesota (47˚30.476'

112 N; 93˚27.1620'W and 412 m a.m.s.l., Figure S1: Map of the Marcell Experimental Forest). Bogs

113 do not have inflow from groundwater and receive inputs only from the atmosphere creating a

114 mineral-poor ombrotrophic peatland [38,39]. Mean annual air temperature at the MEF from 1961 to

115 2019 was 3.5 ℃ and average annual precipitation was 770 mm [40]. Much of the peat is 2 - 4 m deep

116 and the peatland water table fluctuates seasonally within the upper 30 cm of peat during most years

117 [41,42].

118

119 Water flows laterally through a shallow acrotelm and mesotelm to the peatland margin, and an

120 outlet stream when the water table is high [43]. The acrotelm is a surficial layer of low density and

121 comparatively high hydraulic conductivity, is mostly oxic above the water table and includes living

122 plants and the majority of roots [44]. The catotelm is a deeper zone of permanently saturated and

123 higher density peat with lower hydraulic conductivity and permanently anoxic conditions [45,46].

124 Between the acrotelm and catotelm is the mesotelm (approximately 30 – 50 cm below the surface),

125   a transitional area characterized by a fluctuating water table [36,41,46,47]. The mesotelm is periodically

126   oxic, corresponding to low water tables, or anoxic, corresponding to high water tables.

127

128   The S1 bog surface consists of raised hummocks alternating with microtopographical lows called

129   hollows. Typical relief is 20 - 30 cm from hummock tops to adjacent hollows and the lateral extent

130   of hummocks can be up to several meters wide [48,49]. The bryophytes in hummocks consist mainly

131   of *Sphagnum divinum* (previously *S. magellanicum* [50]*),* while hollows are mainly colonized by *S.*

132   *angustifolium* and *S. fallax*. *Sphagnum angustifolium* and *S. fallax* have few, readily

133   distinguishable features so we refer to them as *S. angustifolium/fallax*. The S1 bog is the site of

134   the long-term and large-scale Spruce and Peatland Responses Under Changing Environments

135   (SPRUCE) experiment where air and peat temperatures (0 to +9 °C above ambient) and

136   atmospheric carbon dioxide (CO_2) levels (ambient and +500 ppm) are being manipulated to study

137   climate effects on ecological, hydrological, and biogeochemical processes in peatlands [51]. All data

138   presented in this paper were collected prior to the onset of the experimental warming and elevated

139   CO_2 treatments.

140

141   **2.2 Sampling Methods**

142   Peat cores were collected to a depth of -200 cm from six locations in triplicate for a total of 18

143   cores in August 2012 [48]. See the Supplemental Information for detailed coring, sampling intervals,

144   and sampling methods. Samples for mercury were frozen and samples for sulfur were stored in

145   argon and frozen. Living *Sphagnum divinum* and *S. angustifolium/fallax* were sampled in June

146   2014 and stored frozen before further analyses. Porewaters were collected from piezometers in

147   2013 [52].

148

149   The different sample types were collected at different times but all were collected from the same

150   peat bog. Peat soil was collected in August 2012, porewaters were collected in September 2013,

151   and peat for the rate study was collected in 2016. It is possible that environmental conditions (water

152   table height, temperature) were different between sampling time points. Over the monitoring

153   history of the Marcell Experimental Forest (since 1967) these factors are generally stable and all

154   samples were collected in the same season although different years.

155

156   **2.3 Sulfur Concentration and Speciation in Peatland Soil**

157   Peat and *Sphagnum* samples were dried in a N_2 (g) filled flow-through desiccator. The samples

158   were then homogenized in a N_2 (g) filled glove bag using a ceramic mortar and pestle and liquid

159   nitrogen. Homogenized samples were stored in N_2 (g) filled packs until analysis.

160

161   Total sulfur concentrations of dried and ground subsamples were measured by combustion using

162   a carbon, nitrogen, sulfur Elementar Vario EL analyzer (Elementar Instruments).

163

164   Sulfur XANES data were acquired on beamlines 06B1-1 Soft X-ray Microcharacterization

165   Beamline (SXRMB) at the Canadian Light Source (CLS, Saskatoon, SK, Canada) and 9-BM X-

166   ray beamline at the Advanced Photon Source (APS, Argonne National Laboratory, Argonne, IL,

167   USA). See the Supplemental Information for detailed methods. Sulfur XANES spectra were

168   processed using *Athena* [53]. Linear combination fitting of the sample spectra with reference spectra

169   was performed using *mrfitty* [54]. We used a subset of a published sulfur reference database [55–59]

170   (Table S1: List of sulfur reference compounds).

171

2.4 Acid Volatile Sulfur and Sulfate in Porewaters

Porewaters were analyzed for sulfide concentration by protonating all acid-extractable sulfides to

H_2S (g) and using the methylene blue colorimetric method [60]. The working range for this method

was 0.01 - 2.0 mg L^{-1}.

Porewaters were analyzed for sulfate on a Thermo Dionex ICS-2100 ion chromatograph according

to Standard Method 4110 C [52,61]. The limit of detection was 0.02 mg L^{-1} SO_4^{2-}.

178

2.5 Total Mercury and MeHg Concentration in Peatland Soil

Total mercury (THg) was measured by cold vapor atomic fluorescence spectroscopy (CVAFS) on

a Tekran 2600 according to US Environmental Protection Agency (EPA) method 1631 [62].

Methylmercury concentrations were measured by EPA Method 1630 [63] by distillation, ethylation,

capillary gas chromatography, and CVAFS on a Tekran 2700. The detection limit was 0.03 ng g^{-1}

for THg analyses and 0.006 ng g^{-1} for MeHg analyses.

185

2.6 Instantaneous mercury methylation and demethylation rate constants

Rates were determined by incubating peat with simultaneous additions of enriched-abundance

$^{200}Hg^{2+}$ (94.3%) and Me$^{201}Hg^+$ (84.7%) as outlined in Mitchell and Gilmour (2008) [29].

See Supplemental Information for detailed methods.

190

Analytical quality control and assurance measures can be found in Table S2: Potential rate

constant quality control and assurance measures. Potential rate constants for Hg^{2+} methylation

(k_m) were calculated using the excess concentration of enriched $^{200}Hg^{2+}$ that was methylated over

9

194   the course of the incubation period with respect to the concentration of excess T^{200}Hg in the

195   sample [64,65]. Potential MeHg demethylation rate constants (k_d) were determined assuming first-

196   order reaction kinetics according to Lehnherr et al. (2012) [66].

197

198   **2.7 *hgc*AB Primer Sequencing**

199   Genomic DNA (gDNA) was isolated from the peat samples, quantified using QubitTM (Thermo

200   Fisher Scientific), and assessed for quality with NanoDropTM One (Thermo Fisher Scientific).

201   See Supplemental Information for detailed methods. The gene sequence *hgc*AB was amplified by

202   the method described by Gionfriddo et al. (2020) [67] and clone libraries were created. The

203   environmental clone *hgc*A sequences from this study were previously published as part of a study

204   testing methods for identifying Hg-methylation genes from environmental samples, and are

205   publicly available under the NCBI GenBank accession numbers MT122211 – MT122438 [67].

206   There could be bias in these methods (amplifying, cloning, and sequencing *hgc*A) introduced by

207   the choice of primer sequence. Primer sequences are based on reference *hgc*A from known

208   methylators, and therefore may prefer certain microbial guilds, such as deltas and methanogens

209   over firmicutes and acetogens. The interpretation of the phylogenetic analysis of this data is limited

210   as metabolic groupings of the results were based on taxonomic prefixes and suffixes as opposed

211   to identifying functional genes for sulfate reduction, iron reduction, and methanogenesis. We

212   inferred sulfate reducing mercury methylators based on the phylogenetic placement of the cloned

213   sequence compared to reference sequences of known/predicted mercury methylators. Since the

214   mercury methylation genes have been classified as Deltaproteobacteria, we inferred that the

215   mercury methylators are capable of sulfate reduction. These data are not quantitative and do not

216   tell us whether any of the *hgc* genes were active, if some groups have higher rates of activity than

217   others (e.g., small number of sulfur reducers but high activity), or whether the organisms were

218   alive when the DNA was extracted. Our data simply identified the presence or absence of *hgc*AB

219   genes.

220

221   **2.8 Statistical Analysis**

222   All statistical analyses were performed in R 3.6.3 [68] using package agricolae (v1.3.2; function:

223   LSD.test) [69]. Statistical differences of linear models were determined using Multiple Comparison

224   Least Significant Difference [70], p-adjustment of "none", and a significance level of $p < 0.05$. The

225   Shapiro-Wilks test was used to determine the normality of THg, MeHg, and percent MeHg. No

226   averaging was performed and the data set was comprised of composited cores and all depths. The

227   data were not normal, so we examined relationships between mercury and sulfur species in peat

228   by using Spearman's rank correlation for non-linear and non-parametric data with a significance

229   level of $p < 0.05$.

230

231   **3. RESULTS AND DISCUSSION**

232   **3.1 Depth Profiles in Peatland Soil - Mercury, Sulfur, and *hgc*AB genes**

233   Spectra from 58 samples were fit to reference spectra using linear combination fitting (Table S3:

234   Proportions of sulfur species for hummocks and S4: Proportions of sulfur species for hollows).

235   Representative sulfur XANES spectra are shown in Figure 1.

236

Almost all sulfur detected in the S1 bog peat with sulfur XANES spectroscopy was in an organic

form (Table S5: Mean sulfur speciation by depth). Reduced organic sulfur species (having valence

states of $\leq +1$, Table 1) comprised 42 – 72 % of total sulfur over the full depth profile (+ 20 cm to

-200 cm, Table S5: Mean sulfur speciation by depth) which is consistent with past studies of boreal

peatlands [71]. The oxidized sulfur species (valence states $\geq + 2$) decreased with depth ($p < 0.05$),

while reduced sulfur species (valence states $\leq +1$) increased with depth ($p < 0.05$). The lowest

percentages of reduced sulfur species were observed in surface samples from both hollows (- 5

cm, 48 % on average) and hummocks (+15 cm, 42 % on average; Figure 2 and Table S5: Mean
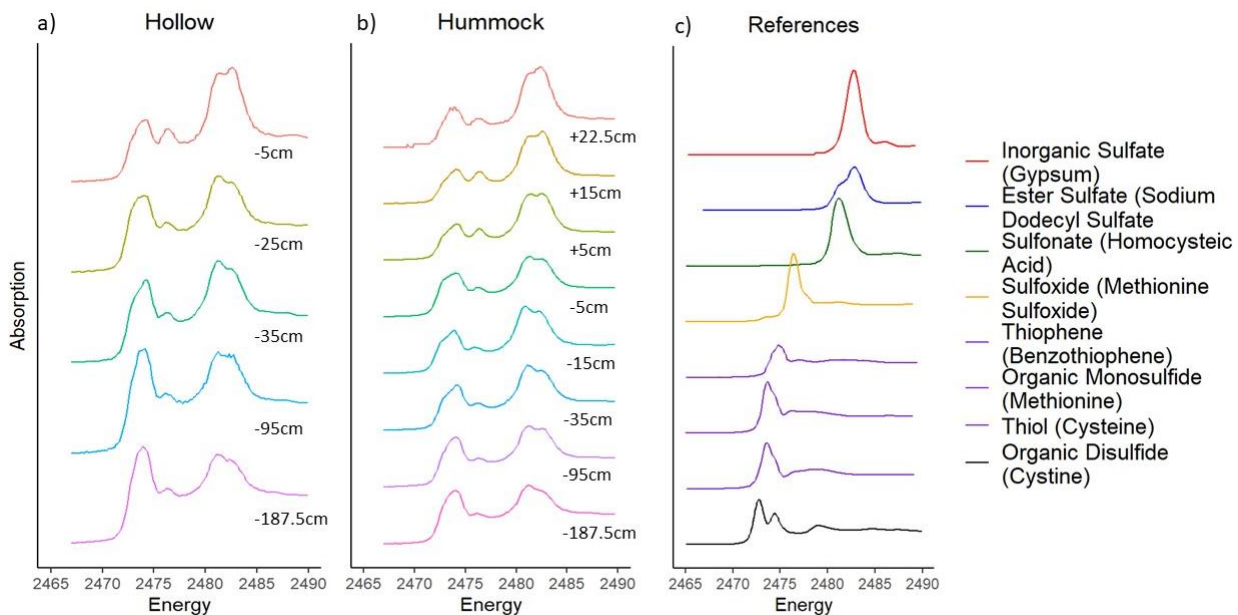
sulfur speciation by depth).

Figure 1 Sulfur 1s X-ray absorption near edge structure (XANES) spectra from a hollow (a), hummock (b), and references that were detected in the samples (c). References are color coded according to bin type – thiophenes, organic monosulfides, and thiols are binned together.

12

Table 1 Sulfur species in the reference database.

Reference compound	Functional group	Structure	Electronic oxidation state	Group	Peak Maxima (eV)	Source
L-Cystine	Organic disulfide	R-S-S-R'	-0.4 [a]		2472.8 / 2474.5	d.
L-Cysteine	Thiol	R-S-H	+0.2		2473.6	d.
L-Methionine	Organic monosulfide	R-S-R'	+0.3	Reduced S	2473.6	d.
Benzothiophene and Bithiophene	Thiophene		+1.0		2473.7 / 2474.6	e., f.
Methionine Sulfoxide	Sulfoxide	R-S(O)-R'	+2		2476.3	d.
Sulfite	Sulfite	$R-SO_3$	+3.68		2478.5 / 2482.1	g., h.
DL-Homocysteic acid [b] and ANSA [c]	Sulfonate	$R-SO_3-H$	+5		2481.2	d., h.
Saccharin	Sulfone	$R-SO_2-R'$	+6	Oxidized S	2480.0	f.
Gypsum	Inorganic sulfate	$CaSO_4$	+6		2482.7	f.
Sodium dodecyl sulfate	Ester sulfate	$R-O-SO_3-H$	+6		2482.8	d.

a. Oxidation state calculated and published in Cron et al. 2020

b. DL-Homocysteic acid

c. 1-Amino-2-naphthol-4-sulfonic acid

d. Cron et al. 2020

e. Behyan et al. 2013

f. Pierce et al. 2021

g. Manceau and Nagy 2012
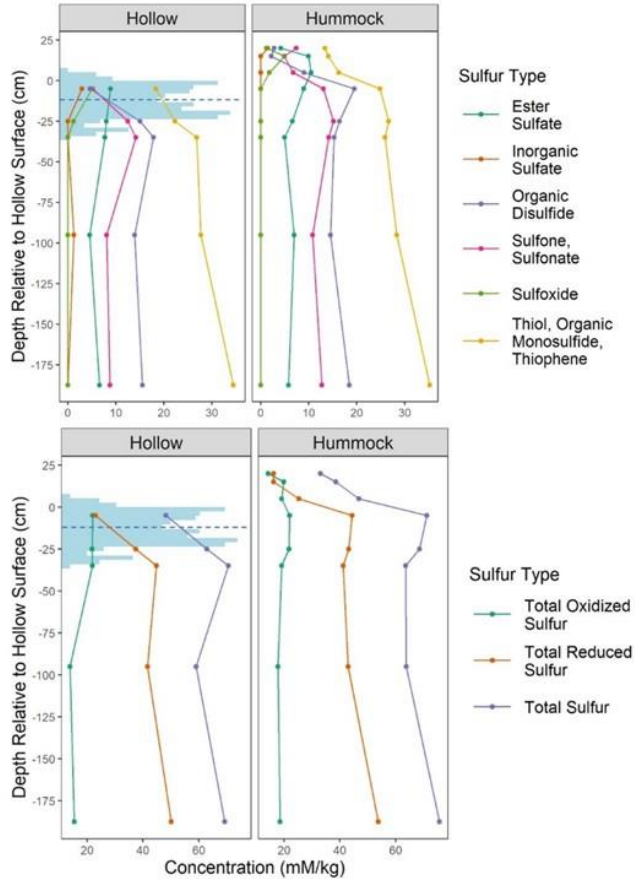
h. Zeng et al. 2013

Figure 2 Depth profiles of sulfur concentration and speciation. Top Panel: Inorganic sulfate (orange), ester sulfate (teal), sulfone and sulfonate (pink), sulfoxide (green), thiol and thiophene and organic monosulfide (yellow), and organic disulfide (purple) as measured by XANES spectroscopy. Bottom Panel: Total oxidized sulfur (teal) is the sum of inorganic sulfate, ester sulfate, sulfone, sulfonate, and sulfoxide. Total reduced sulfur (orange) is the sum of thiol, organic monosulfide, thiophene, and organic disulfide. Blue shaded area is a histogram showing the range of daily water table positions (minimum: -35 cm, maximum: +6 cm) in 2012. Blue dashed line is the water table height on the day of sampling.

Various organic sulfur species with different electronic states (- 0.4 to + 6) were measured in living *Sphagnum* (Table S5: Mean sulfur speciation by depth). Sulfur speciation in *Sphagnum* tissues was similar between *S. divinum* and *S. angustifolium/fallax*. The main difference between the two was that *S. divinum* accumulated more inorganic sulfate, whereas *S. angustifolium/fallax*, accumulated more ester sulfate. However, only one sample per *Sphagnum* type was measured, so the potential variability in sulfur speciation was not addressed.

Within the acrotelm and mesotelm, concentrations of sulfur species were variable and in the catotelm, the concentrations were constant. In this study, our observations are consistent with published literature [31,35] that show that the depth interval from -5 cm to -35 cm is a biogeochemically active zone,

269   which overlaps the range of water table depth fluctuations (Figure 2). Maxima in total sulfur,

270   organic disulfide, THg, MeHg, percent MeHg, and major changes in the composition of the sulfur

14

271 organic compounds all occurred in this zone

272 (Figures 2, 3, and S2: Depth profiles of mean

273 THg and percent MeHg). Subsurface

274 maximum in organic sulfur concentration in

275 peatlands may result from sulfate reduction

276 processes occurring where perennial

277 saturation most often occurs [72]. Our findings

278 are consistent with previous reports of

279 subsurface maxima in total sulfur and MeHg

280 that correspond to the mesotelm [31,35,47,72,73]. It

281 has been proposed that this maximum in

282 MeHg in the zone of water table fluctuation is

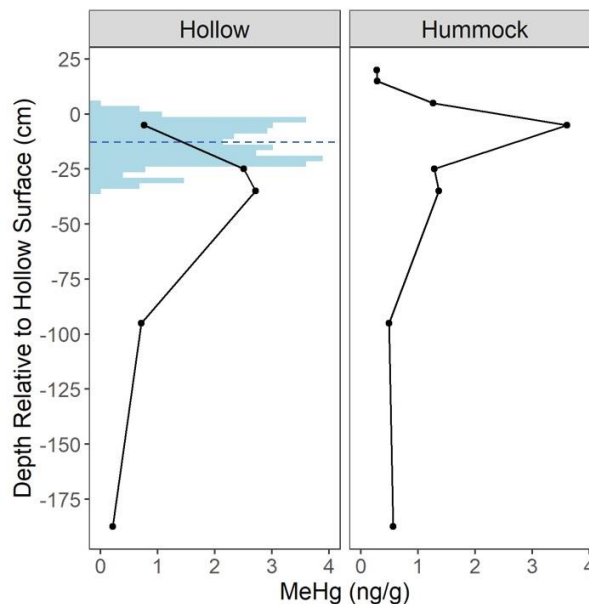283 due to sulfur cycling between reduced and

Figure 3 Depth profile of mean MeHg concentrations in peat for cores collected from hummocks and hollows. Blue shaded area is a histogram of the range of water table positions in 2012. Blue dashed line is the water table height on the day of sampling. Total mercury and percent MeHg depth profiles are provided in the Supplemental Information (Figure S2).

284 oxidized forms as the redox conditions change with the water table [15,32,34,74,75]. This internal cycling

285 of sulfur can drive MeHg production with minimal atmospheric deposition of new sulfate.

286

287 Both THg and MeHg concentrations were relatively low in surficial peat and peaked at depths

288 between -25 cm and -35 cm in the hollows and at -5 cm in the hummocks (Figures 2 and S2: Depth

289 profiles of mean THg and percent MeHg, Table S6: Mean mercury concentrations by depth). The

290 shape of the MeHg profile is directly influenced by microbial activity. In contrast, the shape of the

291 THg profile is determined primarily by atmospheric deposition and indirectly influenced by

292 microbial activity. Mercury emissions greatly increased during the industrial revolution (~1850)

293 through the 1970s [76] which corresponds to increased atmospheric deposition in depths -25 cm to -

294 100 cm (hollows, Figure S2: Depth profiles of mean THg and percent MeHg). Microbial

295 decomposition of the peat increases the concentration of THg by decreasing the mass of carbon

296 and the volume of peat [77]. In the surface depths one cm of peat may correlate to one year of

297 deposition whereas in the deeper peat, one cm may correlate to several hundred years [77]. Total

298 mercury and MeHg concentrations decreased below -35 cm depth (Figures 3 and S2: Depth

299 profiles of mean THg and percent MeHg, Table S6: Mean mercury concentrations by depth). Our

300 hummock, near-surface, THg concentrations were approximately 50 ng g^{-1} which is consistent

301 with a hummock depth profile measured at a similar bog in northern Minnesota by Benoit et al.

302 (1998) as well as having similar depths for concentration maxima [76]. These same similarities, but

303 for hollows, were found with the THg depth profiles in Givelet et al. (2003) located in southern

304 Ontario, Canada [78]. Average percent MeHg levels (i.e., MeHg concentrations expressed as a

305 percentage of THg concentrations) were less than 2.6 % throughout peat cores and peaked at depths

306 -35 cm and -5 cm for hollows and hummocks, respectively.

307

308 No relationship was found between the presence of *hgc*AB genes and the MeHg profile because

309 the *hgc*AB genes are detected at all depths even where MeHg concentrations are low. The data

310 do not provide quantitative information so the overall abundance of hgcAB in the mesotelm is

311 unknown. Many factors may impact MeHg distribution besides the presence of mercury

312 methylators, including their activity and abundance, which were not measured. A recent study

313 showed no significant correlation between the gene abundance of *hgc*AB (qPCR or

314 metagenomic-based methods) and THg or MeHg concentrations across diverse environments

315 such as riverine areas, tidal marshes, and arctic permafrost [79]. Generally, the potential for

316 microbial methylation of mercury appears to be present throughout the peat profile. There are

317 several caveats to these data. First, the methods do not give a quantitative assessment of *hgc*AB

318 genes across depth. Second, no overall measure of biomass was collected to assess microbial

319 abundance. Third, sequencing was not deep enough (i.e., only 5 or so clones per depth) to

320 capture the full diversity in *hgc*A genes that were present in the clone libraries. However, the

321 collation of clones from each depth and sample site gives us a glimpse of mercury methylator

322 diversity at this site. An area for future investigation is to perform metagenomic sequencing

323 techniques or higher throughput sequencing of *hgc*AB amplicons to overcome these caveats.

324

325 **3.2 Organic Disulfide is a Product of Mercury Methylation**

326 The depth profiles of mercury concentrations and sulfur species were consistent among cores for

327 soils having similar microtopography (e.g., all hummock profiles are similar). The most

328 distinguishing feature of all sulfur speciation profiles was a maximum concentration of organic

329 disulfide in near-surface peat (within ~ 30 cm of the surface for both hummocks and hollows;

330 Figure 2). Within the zone of water table fluctuation, concentration maxima of MeHg and organic

331 disulfide co-occur for both hollows and hummocks. Methylmercury and percent MeHg were both

332 positively correlated with organic disulfide throughout the depth profile in hummocks but not

333 hollows ($R_{Spearman} = 0.62$, Table S7: Spearman's correlations between sulfur species and mercury).

334 We performed a statistical correlation analysis and interpret these results based on well-established

335 chemical and biological processes.

336

337 Hummocks are elevated approximately 30 cm above the hollows (Figure 2) but the absolute water

338 table occurs at the same absolute elevation in both, with the result that the surface layers of

339 hummocks are more oxic than in hollows [44,80]. The maxim in MeHg, total sulfur, and organic

340 disulfide concentrations in hummocks and hollows occur at the same depths from the

341 microtopographic surface (-35 cm, Figures 2 and 3). This indicates that the biogeochemical

342 environment (e.g., soil moisture, redox potential, and biophysical properties) in the mesotelm

343 varies with surface microtopography [81]. There may well be a biogeochemical reason for the

344 significant correlation between MeHg and organic disulfide in hummocks, but not hollows. It is

345 also possible that our sampling scheme did not allow us to resolve that relationship in hollows

346 because the sampling interval increased from 10 cm to 60 cm at -35 cm below the hollow surface.

347

348 Microbial sulfate reduction produces chemically reduced forms of sulfur, such as hydrogen sulfide

349 [17,82]. Hydrogen sulfide and other forms of sulfur are known to be reactive with organic matter in a

350 variety of natural settings through processes referred to as sulfurization or sulfidization reactions

351 [26,83–85]. Organic disulfide is a possible end-product of microbial sulfate reduction processes in

352 peatlands and may be a co-product with MeHg [31,72,86]. There is evidence SRB are present at our

353 study site at depths -30 cm to -50 cm [87,88]. The 2014 studies by Lin et al. [87,88] were performed at

354 our research site and was generic to all microorganisms in the peat, meaning it differs from ours

355 in that we selected a subset of microorganisms that had the *hgc*AB gene. Microbes containing the

356 *hgc*AB gene comprise less than 5% of the general microbial community across various

357 environment types [79]. Based on interpreting the *hgc*A phylogenetic classification as sulfate

358 reducers, we saw SRB that contain the genes for mercury methylation, *hgc*AB, at depths +5 cm

359 through -10 cm for the hummock locations only (Figure S3: Depth profile of the presence of

360 *hgc*AB and binned microbiological taxa). Not surprisingly, the majority of the genes detected were

361 binned in the "uncultured" and "other" group and so little information can be gleaned as to what

18

362   geochemical or physico-chemical conditions would allow the organisms possessing these genes to

363   thrive and be biochemically active.

364

365

366

367   **3.3 Thiols, Monosulfides, Thiophenes and Mercury Bioavailability**

368   Unlike organic disulfides, the organic monosulfides (thiols, monosulfides, and thiophenes) were

369   negatively correlated with MeHg ($R_{spearman}$ = -0.60 and -0.51, hollows and hummocks respectively)

370   and displayed a maximum in the catotelm where THg and MeHg are low (Figures 2, 3, S2: Depth

371   profiles of mean THg and percent MeHg, and Table S7: Spearman's correlations between sulfur

372   species and mercury). Thiol functional groups in dissolved and particulate organic pools are known

373   to bind to mercury strongly [20,29,89,90]. Studies using extended X-ray absorption fine structure

374   (EXAFS) spectroscopy show that thiol moieties in organic matter form ligand complexes with

375   Hg(II) and CH_3Hg^+ which increases THg and MeHg storage in peatland soil [20,91–93]. In the aqueous

376   phase, thiols introduced as soluble cysteine desorb Hg(II) from the solid phase into the porewaters

377   [94]. While the chemical affinity between mercury and thiols is well demonstrated, the effect of thiols

378   on MeHg production by microorganisms appears to be species and compound specific. Mercury

379   methylating microorganisms such as *Pseudodesulfovibrio mercurii* ND132 (previously *D.*

380   *desulfuricans* ND132) exhibit enhanced methylation in the presence of all thiols whereas *G.*

381   *sulfurreducens* PCA's methylating ability is enhanced by small molecular thiols (e.g., cysteine and

382   mercaptopropionate) and inhibited by larger molecular thiols (e.g., glutathione and penicillamine)

383   [94–97]. The observed negative correlation between thiols and MeHg in peat is consistent with a

384   reduction in methylation activity in the porewaters in the presence of solid-state thiols. This finding

385　is further supported by the observed negative correlation in the peat between thiols and the ratio

386　of methylation rate constants (k_m) to demethylation rate constants (k_d) ($R_{spearman}$ = -0.37, Table S8:

387　Spearman's correlations between sulfur species and potential methylation rate constants). To our

388　knowledge, this is the first finding of this kind outside of a laboratory setting. For MeHg, it is

389　possible that the strong binding affinity between thiols in peat and Hg(II) causes a reduction in

390　bioavailability for methylation in the porewaters. As opposed to peatland soil, studies of porewater

391　have found a positive relationship between k_m and small molecular thiols [98]. It should be noted that

392　in the deep peat, organic monosulfides are not causing a decrease in MeHg. Methylmercury is low

393　in the catotelm because THg concentrations are low. The deep peat is also characterized by lower

394　microbial activity at depth due to environmental conditions. Organic monosulfides in the peatland

395　soil affecting the bioavailability of mercury in the porewater is likely restricted to the acrotelm and

396　mesotelm.

397

398　**3.4 Ester Sulfate as a Potential Substrate for Sulfur Reducing Mercury Methylators**

399　The depths at which the greatest average methylation rate constant, k_m, occurred was -10 cm to -

400　20 cm and corresponded with the depth of the MeHg concentration maximum (Figures 3 and 4).

401　Within the mesotelm, there was high variability in k_m. The demethylation rate constant is variable

402　among replicates and has no significant differences with depth, so the depth profile can be

403　considered flat (Figure 4). The greatest net methylation potential, based on the ratio of k_m to k_d,

404　would occur at -10 to -20 cm depth whereas the greatest net demethylation potential would occur

405　above and below those depths (Figure 4). Between 2002 and 2012, the water table at the S1 bog is

406　most often located between 0 cm and -30 cm [99].

407   Total mercury concentration and methylation rate

408   constant values are strongly and positively

409   correlated $R_{Spearman} = 0.86$, p-value < 0.05 (Figure

410   S4: THg comparison plots with rate data) and this

411   correlation is consistent with previous findings

412   [100,101]. Total mercury concentration and

413   demethylation rate constant values are moderately

414   and negatively correlated ($R_{Spearman} = -0.41$, p-

415   value < 0.05, Figure S4: THg comparison plots

416   with rate data). Methylmercury concentration and

417   the methylation rate constant values are strongly

418   and positively correlated ($R_{Spearman} = 0.67$, p-value

419   < 0.05, Figure S5: MeHg comparison plots with

420   rate data). This positive correlation is consistent

421   with a past study based in saltwater marshes where

422   the correlation between percent MeHg of THg and

423   the methylation rate constant was $R_{pearson} = 0.80$ [29].

424   Methylmercury concentration and the

425   demethylation rate constant values are weakly and

426   negatively correlated ($R_{Spearman} = -0.39$, p-value $<$

427   0.05, Figure S5: MeHg comparison plots with rate
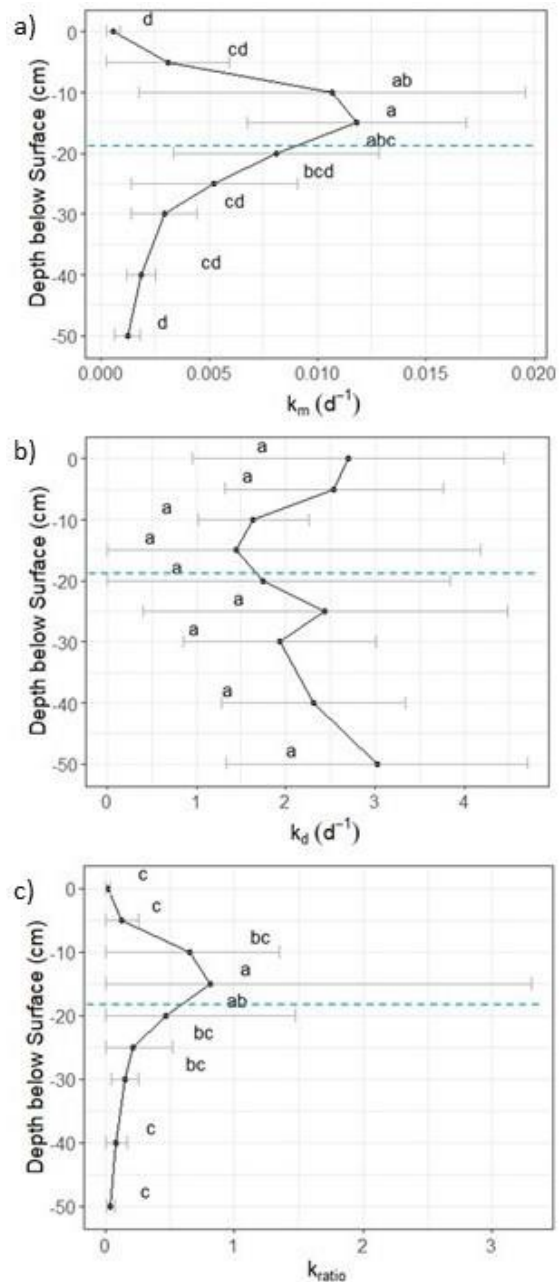
428   data).

429

Figure 4 Rate constant profiles from the S1 bog, August 2016. Rate constant (k_m) is the potential methylation constant (a), k_d is the potential demethylation constant (b), and k_{ratio} is calculated as $k_m \div k_d \times 100$ (c). Error bars are 95% confidence intervals. Means with the same letter are not statistically different from each other ($p \geq 0.05$). Blue dashed line is the water table height on the day of sampling.

21

430   A unique finding in this study is that k_m was positively correlated to total oxidized organic sulfur

431   species and ester sulfate in peat ($R_{spearman}$ = 0.38 and 0.56, respectively). The positive correlation

432   between ester sulfate and k_m provides evidence for ester sulfate being the reactant in the

433   microbially mediated methylation process via sulfate reduction. Inorganic sulfate was present in a

434   few of the samples but was not common (Tables S3: Proportions of sulfur species for hummocks

435   and S4: Proportions of sulfur species for hollows). This finding is consistent with past studies that

436   showed ester sulfate can be utilized by SRB as a terminal electron acceptor in the absence of

437   inorganic sulfate [17,102–104]. Porewater sulfate pools are low (sub-μmol L^{-1}, Figure S6: Depth profiles

438   of mean porewater chemistry) so the positive correlation between k_m and solid phase ester sulfate

439   may indicate that the solid-phase sulfur pools, which have a much larger sulfur concentration

440   range, may be available to microbial activity or exchanging with the porewaters. Congruently, k_m

441   was negatively correlated with total reduced sulfur species ($R_{spearman}$ = -0.38) indicating that as

442   sulfur is reduced, along with producing MeHg, potential methylation rates decrease.

443

444   A variety of biogeochemical pools and processes contribute to the abundance and speciation of

445   sulfur and mercury in an ombrotrophic peatland. Microorganisms and plants immobilize

446   atmospherically deposited sulfate as organic sulfur species through assimilatory and dissimilatory

447   sulfate reduction [105–108]. Sulfate reducing microbes are known to link sulfate reduction to formation

448   of reactive hydrogen sulfide (H_2S_{aq}) and mercury methylation [24,83,109,110]. Several lines of evidence

449   in our findings suggest that dissimilatory sulfate reduction processes were important in the

450   subsurface peat. Porewater sulfate concentrations in hollows revealed a substantial decrease from

451   0 to -50 cm and high variability at -30 cm (Figure S6: Depth profiles of mean porewater chemistry).

452   At the same time, porewater profiles of total dissolved sulfide (H_2S_{aq} and HS^-_{aq}) showed maxima

22

453 at -30 cm suggesting the occurrence of sulfate reduction processes at this depth (Figure S6: Depth

454 profiles of mean porewater chemistry). As MeHg is produced as a co-product with hydrogen

455 sulfide, similar depths of maximum MeHg concentrations and maximum reduced sulfur species

456 are expected and substantiated by our data (Figures 2 and 3). Drying of peatland soils during low

457 water table events may oxidize these organic sulfur compounds and provide sulfate to fuel net

458 MeHg production following subsequent wetting events [15]. Thus, dry-to-wet cycles can liberate

459 sulfate and create the potential for increased MeHg fluxes to surface waters [15,32,111,112].

460

461 Our findings will serve as a time zero characterization of the SPRUCE project, a large-scale

462 temperature and elevated CO_2 manipulation experiment, which was fully initiated in 2016. We

463 anticipate that projected climate changes in the northern hemispheric boreal ecotone will change

464 mercury release from peatlands to downstream aquatic ecosystems and the atmosphere. For

465 instance, climate change and its associated effects on water table fluctuations may drive the

466 subsurface maxima in reduced organic sulfur concentrations, MeHg concentrations, and microbial

467 activity deeper into the peat. The net effect of these changes on mercury fluxes from peatlands

468 under climate warming is currently under investigation.

469

495

Supporting Information

497   Detailed methods and supporting figures/tables are provided in the SI. This material is

498   available free of charge via the Internet at http://pubs.acs.org.

499

REFERENCES

(1)   Yu, Z.; Loisel, J.; Brosseau, D. P.; Beilman, D. W.; Hunt, S. J. Global Peatland Dynamics since the Last Glacial Maximum. *Geophys. Res. Lett.* **2010**, *37* (L13402), 1–5. https://doi.org/10.1029/2010GL043584.

(2)   Krause, L.; McCullough, K. J.; Kane, E. S.; Kolka, R. K.; Chimner, R. A.; Lilleskov, E. A. Impacts of Historical Ditching on Peat Volume and Carbon in Northern Minnesota USA Peatlands. *J. Environ. Manage.* **2021**, *296* (113090), 1–10. https://doi.org/10.1016/j.jenvman.2021.113090.

(3)   Grigal, D. F. Mercury Sequestration in Forests and Peatlands: A Review. *J. Environ. Qual.* **2003**, *32* (2), 393–405. https://doi.org/10.2134/jeq2003.3930.

(4)   Mitchell, C. P. J.; Branfireun, B. A.; Kolka, R. K. Spatial Characteristics of Net Methylmercury Production Hot Spots in Peatlands. *Environ. Sci. Technol.* **2008**, *42* (4), 1010–1016. https://doi.org/10.1021/es0704986.

(5)   Kolka, R. K.; Sebestyen, S. D.; Verry, E. S.; Brooks, K. N. Mercury Cycling in Peatland Watersheds in Peatland Biogeochemistry and Watershed Hydrology. In *Peatland Biogeochemistry and Watershed Hydrology at the Marcell Experimental Forest*; 2011; pp 349–370.

(6)   Ullrich, S. M.; Tanton, T. W.; Abdrashitova, S. A. Mercury in the Aquatic Environment: A Review of Factors Affecting Methylation. *Crit. Rev. Environ. Sci. Technol.* **2001**, *31* (3), 241–293. https://doi.org/10.1080/20016491089226.

(7)   Gilmour, C. C.; Podar, M.; Bullock, A. L.; Graham, A. M.; Brown, S. D.; Somenahally, A. C.; Johs, A.; Hurt, R. A.; Bailey, K. L.; Elias, D. A. Mercury Methylation by Novel Microorganisms from New Environments. *Environ. Sci. Technol.* **2013**, *47*, 11810–11820. https://doi.org/10.1021/es403075t.

(8)   Jeremiason, J. D.; Engstrom, D. R.; Swain, E. B.; Nater, E. A.; Johnson, B. M.; Almendinger, J. E.; Monson, B. A.; Kolka, R. K. Sulfate Addition Increases Methylmercury Production in an Experimental Wetland. *Environ. Sci. Technol.* **2006**, *40* (12), 3800–3806. https://doi.org/10.1021/es0524144.

(9)   Coleman Wasik, J. K.; Mitchell, C. P. J.; Engstrom, D. R.; Swain, E. B.; Monson, B. A.; Balogh, S. J.; Jeremiason, J. D.; Branfireun, B. A.; Eggert, S. L.; Kolka, R. K.; Almendinger, J. E. Methylmercury Declines in a Boreal Peatland When Experimental Sulfate Deposition Decreases. *Environ. Sci. Technol.* **2012**, *46* (12), 6663–6671. https://doi.org/10.1021/es300865f.

(10)   Poulain, A. J.; Barkay, T. Cracking the Mercury Methylation Code. *Science (80-.).* **2013**, *339* (6125), 1280–1281. https://doi.org/10.1126/science.1235591.

(11)   Kronberg, R. M.; Schaefer, J. K.; Björn, E.; Skyllberg, U. Mechanisms of Methyl Mercury Net Degradation in Alder Swamps: The Role of Methanogens and Abiotic Processes. *Environ. Sci. Technol. Lett.* **2018**, *5*, 220–225. https://doi.org/10.1021/acs.estlett.8b00081.

(12)   Bae, H. S.; Dierberg, F. E.; Ogram, A. Periphyton and Flocculent Materials Are Important Ecological Compartments Supporting Abundant and Diverse Mercury Methylator Assemblages in the Florida Everglades. *Appl. Environ. Microbiol.* **2019**, *85* (13), 1–17. https://doi.org/10.1128/AEM.00156-19.

(13)   Regnell, O.; Watras, C. J. Microbial Mercury Methylation in Aquatic Environments: A Critical Review of Published Field and Laboratory Studies. *Environ. Sci. Technol.* **2019**, *53*, 4–19. https://doi.org/10.1021/acs.est.8b02709.

(14)   Qian, C.; Chen, H.; Johs, A.; Lu, X.; An, J.; Pierce, E. M.; Parks, J. M.; Elias, D. A.;

546   Hettich, R. L.; Gu, B. Quantitative Proteomic Analysis of Biological Processes and
547   Responses of the Bacterium Desulfovibrio Desulfuricans ND132 upon Deletion of Its
548   Mercury Methylation Genes. *Proteomics* **2018**, *18* (1700479), 1–12.
549   https://doi.org/10.1002/pmic.201700479.

550 (15) Coleman Wasik, J. K.; Engstrom, D. R.; Mitchell, C. P. J.; Swain, E. B.; Monson, B. A.;
551   Balogh, S. J.; Jeremiason, J. D.; Branfireun, B. A.; Kolka, R. K.; Almendinger, J. E. The
552   Effects of Hydrologic Fluctuation and Sulfate Regeneration on Mercury Cycling in an
553   Experimental Peatland. *J. Geophys. Res. Biogeosciences* **2015**, *120*, 1697–1715.
554   https://doi.org/10.1002/2015JG002993.

555 (16) Kolka, R. K.; Grigal, D. F.; Nater, E. A.; Verry, E. S. Hydrologic Cycling of Mercury and
556   Organic Carbon in a Forested Upland–Bog Watershed. *Soil Sci. Soc. Am. J.* **2001**, *65* (3),
557   897–905. https://doi.org/10.2136/sssaj2001.653897x.

558 (17) Pester, M.; Knorr, K.; Friedrich, M. W.; Wagner, M.; Loy, A. Sulfate-Reducing
559   Microorganisms in Wetlands – Fameless Actors in Carbon Cycling and Climate Change.
560   *Front. Microbiol.* **2012**, *3* (72), 1–19. https://doi.org/10.3389/fmicb.2012.00072.

561 (18) Åkerblom, S.; Bishop, K.; Björn, E.; Lambertsson, L.; Eriksson, T.; Nilsson, M. B.
562   Significant Interaction Effects from Sulfate Deposition and Climate on Sulfur
563   Concentrations Constitute Major Controls on Methylmercury Production in Peatlands.
564   *Geochim. Cosmochim. Acta* **2013**, *102*, 1–11. https://doi.org/10.1016/j.gca.2012.10.025.

565 (19) Nagy, K. L.; Manceau, A.; Gasper, J. D.; Ryan, J. N.; Aiken, G. R. Metallothionein-Like
566   Multinuclear Clusters of Mercury (II) and Sulfur in Peat. *Environ. Sci. Technol.* **2011**, *45*,
567   7298–7306. https://doi.org/10.1021/es201025v.

568 (20) Manceau, A.; Nagy, K. L. Relationships between Hg(II)-S Bond Distance and Hg(II)
569   Coordination in Thiolates. *Dalt. Trans.* **2008**, *11* (11), 1421–1425.
570   https://doi.org/10.1039/b718372k.

571 (21) Skyllberg, U. Competition among Thiols and Inorganic Sulfides and Polysulfides for Hg
572   and MeHg in Wetland Soils and Sediments under Suboxic Conditions: Illumination of
573   Controversies and Implications for MeHg Net Production. *J. Geophys. Res.* **2008**, *113*, 1–
574   14. https://doi.org/10.1029/2008JG000745.

575 (22) Mitchell, C. P. J.; Branfireun, B. A.; Kolka, R. K. Assessing Sulfate and Carbon Controls
576   on Net Methylmercury Production in Peatlands: An in Situ Mesocosm Approach. *Appl.*
577   *Geochemistry* **2008**, *23*, 503–518. https://doi.org/10.1016/j.apgeochem.2007.12.020.

578 (23) Åkerblom, S.; Nilsson, M. B.; Skyllberg, U.; Bjorn, E.; Jonsson, S.; Ranneby, B.; Bishop,
579   K. Formation and Mobilization of Methylmercury across Natural and Experimental Sulfur
580   Deposition Gradients. *Environ. Pollut.* **2020**, *263*, 1–12.
581   https://doi.org/10.1016/j.envpol.2020.114398.

582 (24) Blodau, C.; Mayer, B.; Peiffer, S.; Moore, T. R. Support for an Anaerobic Sulfur Cycle in
583   Two Canadian Peatland Soils. *J. Geophys. Res.* **2007**, *112*, 1–10.
584   https://doi.org/10.1029/2006JG000364.

585 (25) Urban, N.; Eisenreich, S.; Grigal, D. F. Sulfur Cycling in a Forested Sphagnum Bog in
586   Northern Minnesota. *Biogeochemistry* **1989**, *7*, 81–109.

587 (26) Fakhraee, M.; Li, J.; Katsev, S. Significant Role of Organic Sulfur in Supporting
588   Sedimentary Sulfate Reduction in Low-Sulfate Environments. *Geochim. Cosmochim. Acta*
589   **2017**, *213*, 502–516. https://doi.org/10.1016/j.gca.2017.07.021.

590 (27) Jochum, L. M.; Schreiber, L.; Marshall, I. P. G.; Jørgensen, B. B.; Schramm, A.; Kjeldsen,
591   K. U. Single-Cell Genomics Reveals a Diverse Metabolic Potential of Uncultivated

592   Desulfatiglans-Related Deltaproteobacteria Widely Distributed in Marine Sediment.
593   *Front. Microbiol.* **2018**, *9* (2039), 1–16. https://doi.org/10.3389/fmicb.2018.02038.

594 (28) Parks, J. M.; Johs, A.; Podar, M.; Bridou, R.; Hurt, R. A.; Smith, S. D.; Tomanicek, S. J.;
595   Qian, Y.; Brown, S. D.; Brandt, C. C.; Palumbo, A. V.; Smith, J. C.; Wall, J. D.; Elias, D.
596   A.; Liang, L. The Genetic Basis for Bacterial Mercury Methylation. *Science (80-.).* **2013**,
597   *339* (6125), 1332–1335. https://doi.org/10.1126/science.1230667.

598 (29) Mitchell, C. P. J.; Gilmour, C. C. Methylmercury Production in a Chesapeake Bay Salt
599   Marsh. *J. Geophys. Res.* **2008**, *113* (G00C04), 1–14.
600   https://doi.org/10.1029/2008JG000765.

601 (30) Coleman Wasik, J. K.; Engstrom, D. R.; Mitchell, C. P. J.; Swain, E. B.; Monson, B. A.;
602   Balogh, S. J.; Jeremiason, J. D.; Branfireun, B. A.; Kolka, R. K.; Almendinger, J. E. The
603   Effects of Hydrologic Fluctuation and Sulfate Regeneration on Mercury Cycling in an
604   Experimental Peatland. *J. Geophys. Res. Biosci.* **2015**, 1697–1715.
605   https://doi.org/10.1002/2015JG002993.

606 (31) Novak, M.; Wieder, R. K. Inorganic and Organic Sulfur Profiles in Nine Sphagnum Peat
607   Bogs in the United States and Czechoslovakia. *Water Air Soil Pollut.* **1992**, *65*, 353–369.

608 (32) Rolfhus, K. R.; Hurley, J. P.; Bodaly, R. A. D.; Perrine, G. Production and Retention of
609   Methylmercury in Inundated Boreal Forest Soils. *Environ. Sci. Technol.* **2015**, *49*, 3482–
610   3489. https://doi.org/10.1021/es505398z.

611 (33) Haynes, K. M.; Kane, E. S.; Potvin, L.; Lilleskov, E. A.; Kolka, R. K.; Mitchell, C. P. J.
612   Gaseous Mercury Fluxes in Peatlands and the Potential Influence of Climate Change.
613   *Atmos. Environ.* **2017**, *154*, 247–259. https://doi.org/10.1016/j.atmosenv.2017.01.049.

614 (34) Haynes, K. M.; Kane, E. S.; Potvin, L.; Lilleskov, E. A.; Kolka, R. K.; Mitchell, C. P. J.
615   Mobility and Transport of Mercury and Methylmercury in Peat as a Function of Changes
616   in Water Table Regime and Plant Functional Groups. *Global Biogeochem. Cycles* **2017**,
617   *31* (2), 233–244. https://doi.org/10.1002/2016GB005471.

618 (35) Haynes, K. M.; Kane, E. S.; Potvin, L.; Lilleskov, E. A.; Kolka, R. K.; Mitchell, C. P. J.
619   Impacts of Experimental Alteration of Water Table Regime and Vascular Plant
620   Community Composition on Peat Mercury Profiles and Methylmercury Production. *Sci.*
621   *Total Environ.* **2019**, *682*, 611–622. https://doi.org/10.1016/j.scitotenv.2019.05.072.

622 (36) Sirota, J. I.; Kolka, R. K.; Sebestyen, S. D.; Nater, E. A. Mercury Dynamics in the Pore
623   Water of Peat Columns during Experimental Freezing and Thawing. *J. Environ. Qual.*
624   **2020**, *49*, 404–416. https://doi.org/10.1002/jeq2.20046.

625 (37) Shi, X.; Thornton, P. E.; Ricciuto, D. M.; Hanson, P. J.; Mao, J.; Sebestyen, S. D.;
626   Griffiths, N. A.; Bisht, G. Representing Northern Peatland Microtopography and
627   Hydrology within the Community Land Model. *Biogeosciences* **2015**, *12*, 6463–6477.
628   https://doi.org/10.5194/bg-12-6463-2015.

629 (38) Gorham, E. Biotic Impoverishment in Northern Peatlands. In *Earth in Transition:*
630   *Patterns and Process of Biotic Impoverishment*; Woodwell, G. M., Ed.; Cambridge
631   University Press: New York, 1990; pp 65–98.

632 (39) Glaser, P. H. *The Ecology of Petterned Boreal Peatlands of Northern Minnesota*; 1987.

633 (40) Sebestyen, S. D.; Lany, N. K.; Roman, D. T.; Burdick, J. M.; Kyllander, R. L.; Verry, E.
634   S.; Kolka, R. K. Hydrological and Meteorological Data from Research Catchments at the
635   Marcell Experimental Forest. *Hydrol. Process.* **2021**, *35* (:e14092), 1–9.
636   https://doi.org/10.1002/hyp.14092.

637 (41) Sebestyen, S. D.; Dorrance, C.; Olson, D. M.; Verry, E. S.; Kolka, R. K.; Elling, A. E.;

638   Kyllander, R. Long-Term Monitoring Sites and Trends at the Marcell Experimental
639   Forest. In *Peatland biogeochemistry and watershed hydrology at the Marcell*
640   *Experimental Forest*; 2011; pp 15–71.

641 (42) Parsekian, A. D.; Slater, L.; Nolan, J.; Kolka, R. K.; Hanson, P. J. Uncertainty in Peat
642   Volume and Soil Carbon Estimated Using Ground-Penetrating Radar and Probing. *Soil*
643   *Sci. Soc. Am. J.* **2012**, *76*, 1911–1918. https://doi.org/10.2136/sssaj2012.0040.

644 (43) Verry, E. S.; Brooks, K. N.; Nichols, D. S.; Ferris, D. R.; Sebestyen, S. D. Watershed
645   Hydrology. In *Peatland Biogeochemistry and Watershed Hydrology at the Marcell*
646   *Experimental Forest*; 2011; pp 193–212.

647 (44) Nungesser, M. K. Modelling Microtopography in Boreal Peatlands: Hummocks and
648   Hollows. *Ecol. Modell.* **2003**, *165*, 175–207. https://doi.org/10.1016/S0304-
649   3800(03)00067-X.

650 (45) Verry, E. S.; Boelter, D. H.; Päivänen, J.; Nichols, D. S.; Malterer, T.; Gafni, A. Physical
651   Properties of Organic Soils. In *Peatland Biogeochemistry and Watershed Hydrology at the*
652   *Marcell Experimental Forest*; 2011; pp 135–176.

653 (46) Tfaily, M. M.; Cooper, W. T.; Kostka, J. E.; Chanton, P. R.; Schadt, C. W.; Hanson, P. J.;
654   Iversen, C. M.; Chanton, J. P. Organic Matter Transformation in the Peat Column at
655   Marcell Experimental Forest: Humification and Vertical Stratification. *J. Geophys. Res.*
656   *Biogeosciences* **2014**, 661–675. https://doi.org/10.1002/2015JG002993.

657 (47) Clymo, R. S.; Bryant, C. L. Diffusion and Mass Flow of Dissolved Carbon Dioxide ,
658   Methane , and Dissolved Organic Carbon in a 7-m Deep Raised Peat Bog. *Geochim.*
659   *Cosmochim. Acta* **2008**, *72*, 2048–2066. https://doi.org/10.1016/j.gca.2008.01.032.

660 (48) Iversen, C. M.; Hansen, P.; Brice, D. J.; Phillips, J. R.; Mcfarlane, K. J.; Hobbie, E. A.;
661   Kolka, R. K. SPRUCE Peat Physical and Chemical Characteristics from Experimental
662   Plot Cores , 2012. *Carbon Dioxide Inf. Anal. Center, Oak Ridge Natl. Lab. U.S. Dep.*
663   *Energy, Oak Ridge, Tennessee, U.S.A.* **2014**.

664 (49) Graham, J. D.; Glenn, N. F.; Spaete, L. P.; Hanson, P. J. Characterizing Peatland
665   Microtopography Using Gradient and Microform-Based Approaches. *Ecosystems* **2020**,
666   *23*, 1464–1480. https://doi.org/10.1007/s10021-020-00481-z.

667 (50) Hassel, K.; Kyrkjeeide, M. O.; Yousefi, N.; Prestø, T.; Stenøien, H. K.; Shaw, J. A.;
668   Flatberg, K. I. Sphagnum Divinum (Sp. Nov.) and S. Medium Limpr. and Their
669   Relationship to S. Magellanicum Brid. *J. Bryol.* **2018**, *40* (3), 197–222.
670   https://doi.org/10.1080/03736687.2018.1474424.

671 (51) Hanson, P. J.; Riggs, J. S.; Robert Nettles, W.; Phillips, J. R.; Krassovski, M. B.; Hook, L.
672   A.; Gu, L.; Richardson, A. D.; Aubrecht, D. M.; Ricciuto, D. M.; Warren, J. M.; Barbier,
673   C. Attaining Whole-Ecosystem Warming Using Air and Deep-Soil Heating Methods with
674   an Elevated CO2 Atmosphere. *Biogeosciences* **2017**, *14* (4), 861–883.
675   https://doi.org/10.5194/bg-14-861-2017.

676 (52) Griffiths, N. A.; Sebestyen, S. D. SPRUCE Porewater Chemistry Data for Experimental
677   Plots Beginning in 2013. *Oak Ridge, TN Carbon Dioxide Inf. Anal. Center, Oak Ridge*
678   *Natl. Lab. U.S. Dep. Energy* **2016**, 1–15.

679 (53) Ravel, B.; Newville, M. ATHENA, ARTEMIS, HEPHAESTUS: Data Analysis for X-Ray
680   Absorption Spectroscopy Using IFEFFIT. *J. Synchrotron Radiat.* **2005**, *12*, 537–541.
681   https://doi.org/10.1107/S0909049505012719.

682 (54) Nicholas, S. L.; Erickson, M. L.; Woodruff, L. G.; Knaeble, A. R.; Marcus, M. A.; Lynch,
683   J. K.; Toner, B. M. Solid-Phase Arsenic Speciation in Aquifer Sediments: A Micro-X-Ray

684   Absorption Spectroscopy Approach for Quantifying Trace-Level Speciation. *Geochim.*
685   *Cosmochim. Acta* **2017**, *211*, 228–255. https://doi.org/10.1016/j.gca.2017.05.018.

686 (55)   Cron, B. R.; Sheik, C. S.; Kafantaris, F. C. A.; Druschel, G. K.; Seewald, J. S.; German,
687   C. R.; Dick, G. J.; Breier, J. A.; Toner, B. M. Dynamic Biogeochemistry of the Particulate
688   Sulfur Pool in a Buoyant Deep-Sea Hydrothermal Plume. *ACS Earth Sp. Chem.* **2020**, *4*
689   (2), 168–182. https://doi.org/10.1021/acsearthspacechem.9b00214.

690 (56)   Zeng, T.; Arnold, W. A.; Toner, B. M. Microscale Characterization of Sulfur Speciation in
691   Lake Sediments. *Environ. Sci. Technol.* **2013**, *47*, 1287–1296.
692   https://doi.org/10.1021/es303914q.

693 (57)   Manceau, A.; Nagy, K. L. Quantitative Analysis of Sulfur Functional Groups in Natural
694   Organic Matter by XANES Spectroscopy. *Geochim. Cosmochim. Acta* **2012**, *99*, 206–223.
695   https://doi.org/10.1016/j.gca.2012.09.033.

696 (58)   Burton, E. D.; Bush, R. T.; Sullivan, L. A.; Hocking, R. K.; Mitchell, D. R. G.; Johnston,
697   S. G.; Fitzpatrick, R. W.; Raven, M.; McClure, S.; Jang, L. Y. Iron-Monosulfide
698   Oxidation in Natural Sediments: Resolving Microbially Mediated S Transformations
699   Using XANES, Electron Microscopy, and Selective Extractions. *Environ. Sci. Technol.*
700   **2009**, *43* (9), 3128–3134. https://doi.org/10.1021/es8036548.

701 (59)   Behyan, S.; Hu, Y.; Urquhart, S. G. Sulfur 1 s near Edge X-Ray Absorption Fine Structure
702   Spectroscopy of Thiophenic and Aromatic Thioether Compounds. *J. Chem. Phys.* **2013**,
703   *138* (214302), 0–11. https://doi.org/10.1063/1.4807604.

704 (60)   4500-S2- D Methylene Blue Method http://standardmethods.org/.

705 (61)   APHA. *Standard Methods for the Examination of Water and Wastewater*, 23rd ed.;
706   American Public Health Association: Washington DC, USA, 2017.

707 (62)   U.S. Environmental Protection Agency. Method 1631, Revision E: Mercury in Water by
708   Oxidation, Purge and Trap, and Cold Vapor Atomic Fluorescence Spectrometry. *EPA*
709   *821-R-96-012* **2002**, 1–46.

710 (63)   U.S. Environmental Protection Agency. Method 1630, Methyl Mercury in Water by
711   Distillation, Aqueous Ethylation, Purge and Trap, and Cold-Vapor Atomic Fluorescence
712   Spectrometry. *EPA-821-R-01-020* **1998**, 1–46.

713 (64)   Hintelmann, H.; Ogrinc, N. Determination of Stable Mercury Isotopes by ICP/MS and
714   Their Application in Environmental Studies. In *Biogeochemistry of Environmentally*
715   *Important Trace Elements*; American Chemical Society: Washington DC, USA, 2003; pp
716   321–338. https://doi.org/10.1021/bk-2003-0835.ch021.

717 (65)   Hintelmann, H.; Evans, R. D.; Villeneuve, J. Y. Measurement of Mercury Methylation in
718   Sediments by Using Enriched Stable Mercury Isotopes Combined with Methylmercury
719   Determination by Gas Chromatography-Inductively Coupled Plasma Mass Spectrometry.
720   *J. Anal. At. Spectrom.* **1995**, *10*, 619–624. https://doi.org/10.1039/JA9951000619.

721 (66)   Lehnherr, I.; St. Louis, V. L.; Emmerton, C. A.; Barker, J. D.; Kirk, J. L. Methylmercury
722   Cycling in High Arctic Wetland Ponds: Sources and Sinks. *Environ. Sci. Technol.* **2012**,
723   *46* (19), 10514–10522. https://doi.org/10.1021/es300576p.

724 (67)   Gionfriddo, C. M.; Wymore, A. M.; Jones, D. S.; Wilpiszeski, R. L.; Lynes, M. M.;
725   Christensen, G. A.; Soren, A.; Gilmour, C. C.; Podar, M.; Elias, D. A. An Improved
726   HgcAB Primer Set and Direct High-Throughput Sequencing Expand Hg-Methylator
727   Diversity in Nature. *Front. Microbiol.* **2020**, *11* (541554), 1–23.
728   https://doi.org/10.3389/fmicb.2020.541554.

729 (68)   R Core Team. R: A Language and Environment for Statistical Computing. *R: A language*

730   *and environment for statistical computing*. R Foundation for Statistical Computing:
731   Vienna, Austria 2017.

732 (69) de Mendiburu, F.; Yaseen, M. Agricolae: Statistical Procedures for Agricultural Research.
733   2020.

734 (70) Steel, R. G. D.; Torrie, J. H.; Dickey, D. A. *Principles and Procedures of Statistic a*
735   *Biometrical Approach*, Third.; The McGraw Hill Companies, Inc., 1997.

736 (71) Skyllberg, U.; Qian, J.; Frech, W.; Xia, K.; Bleam, W. F. Distribution of Mercury, Methyl
737   Mercury and Organic Sulphur Species in Soil, Soil Solution and Stream of a Boreal Forest
738   Catchment. *Biogeochemistry* **2003**, *64*, 53–76. https://doi.org/10.1023/A:1024904502633.

739 (72) Novak, M.; Buzek, F.; Adamova, M. Vertical Trends in 13C, 15N and 34S Ratios in Bulk
740   Sphagnum Peat. *Soil Biol. Biochem.* **1999**, *31*, 1343–1346.

741 (73) Vile, M. A.; Novak, M. Sulfur Cycling in Boreal Peatlands: From Acid Rain to Global
742   Climate Change. In *Boreal Peatland Ecosystems*; Springer Berline Heidelberg, 2006.

743 (74) McCarter, C. P. R.; Branfireun, B. A.; Price, J. S. Nutrient and Mercury Transport in a
744   Sub-Arctic Ladder Fen Peatland Subjected to Simulated Wastewater Discharges. *Sci.*
745   *Total Environ.* **2017**, *609*, 1349–1360. https://doi.org/10.1016/j.scitotenv.2017.07.225.

746 (75) Wang, B.; Nilsson, M. B.; Eklöf, K.; Hu, H.; Ehnvall, B.; Bravo, A. G.; Zhong, S.;
747   Åkeblom, S.; Björn, E.; Bertilsson, S.; Skyllberg, U.; Bishop, K. Opposing Spatial Trends
748   in Methylmercury and Total Mercury along a Peatland Chronosequence Trophic Gradient.
749   *Sci. Total Environ.* **2020**, *718* (13706), 1–9.
750   https://doi.org/10.1016/j.scitotenv.2020.137306.

751 (76) Benoit, J. M.; Fitzgerald, W. F.; Damman, A. W. H. The Biogeochemistry of an
752   Ombrotrophic Bog: Evaluation of Use as an Archive of Atmospheric Mercury Deposition.
753   *Environ. Res.* **1998**, *78* (ER983850), 118–133. https://doi.org/10.1006/enrs.1998.3850.

754 (77) Fissore, C.; Nater, E. A.; McFarlane, K. J.; Klein, A. S. Decadal Carbon Decomposition
755   Dynamics in Three Peatlands in Northern Minnesota. *Biogeochemistry* **2019**, *145*, 63–79.
756   https://doi.org/10.1007/s10533-019-00591-4.

757 (78) Givelet, N.; Roos-Barraclough, F.; Shotyk, W. Predominant Anthropogenic Sources and
758   Rates of Atmospheric Mercury Accumulation in Southern Ontario Recorded by Peat
759   Cores from Three Bogs: Comparison with Natural "Background" Values (Past 8000
760   Years). *J. Environ. Monit.* **2003**, *5*, 935–949. https://doi.org/10.1039/b307140e.

761 (79) Christensen, G. A.; Gionfriddo, C. M.; King, A. J.; Moberly, J. G.; Miller, C. L.;
762   Somenahally, A. C.; Callister, S. J.; Brewer, H.; Podar, M.; Brown, S. D.; Palumbo, A. V;
763   Brandt, C. C.; Wymore, A. M.; Brooks, S. C.; Hwang, C.; Fields, M. W.; Wall, J. D.;
764   Gilmour, C. C.; Elias, D. A. Determining the Reliability of Measuring Mercury Cycling
765   Gene Abundance with Correlations with Mercury and Methylmercury Concentrations.
766   *Environ. Sci. Technol.* **2019**, *53*, 8649–8663. https://doi.org/10.1021/acs.est.8b06389.

767 (80) Santelmann, M. V. Cellulose Mass Loss in Ombrotrophic Bogs of Northeastern North
768   America. *Can. J. Bot.* **1992**, *70*, 2378–2383.

769 (81) Branfireun, B. A. Does Microtopography Influence Subsurface Porewater Chemistry?
770   Implications for the Study of Methylmercury in Peatlands. *Wetlands* **2004**, *24* (1), 207–
771   211.

772 (82) Mandernack, K. W.; Lynch, L.; Krouse, H. R.; Morgan, M. D. Sulfur Cycling in Wetland
773   Peat of the New Jersey Pinelands and Its Effect on Stream Water Chemistry. *Geochim.*
774   *Cosmochim. Acta* **2000**, *64* (23), 3949–3964. https://doi.org/10.1016/S0016-
775   7037(00)00491-9.

776 (83) Einsiedl, F.; Mayer, B.; Schäfer, T. Evidence for Incorporation of H2S in Groundwater
777   Fulvic Acids from Stable Isotope Ratios and Sulfur K-Edge X-Ray Absorption Near Edge
778   Structure Spectroscopy. *Environ. Sci. Technol.* **2008**, *42*, 2439–2444.

779 (84) Heitmann, T.; Blodau, C. Oxidation and Incorporation of Hydrogen Sulfide by Dissolved
780   Organic Matter. *Chem. Geol.* **2006**, *235*, 12–20.
781   https://doi.org/10.1016/j.chemgeo.2006.05.011.

782 (85) Hoffman, M.; Mikutta, C.; Kretzschmar, R. Bisulfide Reaction with Natural Organic
783   Matter Enhances Arsenite Sorption: Insights from X- Ray Absorption Spectroscopy.
784   *Environ. Sci. Technol.* **2012**, *46*, 11788–11797.

785 (86) Novak, M.; Bottrell, S. H.; Prechova, E. Sulfur Isotope Inventories of Atmospheric
786   Deposition , Spruce Forest Floor and Living Sphagnum along a NW-SE Transect across
787   Europe. *Biogeochemistry* **2001**, *53*, 23–50.

788 (87) Lin, X.; Tfaily, M. M.; Green, S. J.; Steinweg, J. M.; Chanton, P.; Imvittaya, A.; Chanton,
789   J. P.; Cooper, W.; Schadt, C.; Kostka, J. E. Microbial Metabolic Potential for Carbon
790   Degradation and Nutrient (Nitrogen and Phosphorus) Acquisition in an Ombrotrophic
791   Peatland. *Am. Soc. Microbiol.* **2014**, *80* (11), 3531–3540.
792   https://doi.org/10.1128/AEM.00206-14.

793 (88) Lin, X.; Tfaily, M. M.; Steinweg, J. M.; Chanton, P.; Esson, K.; Yang, Z. K.; Chanton, J.
794   P.; Cooper, W.; Schadt, C. W.; Kostka, J. E. Microbial Community Stratification Linked
795   to Utilization of Carbohydrates and Phosphorus Limitation in a Boreal Peatland at Marcel
796   Experimental Forest, Minnesota, USA. *Am. Soc. Microbiol.* **2014**, *80* (11), 3518–3530.
797   https://doi.org/10.1128/AEM.00205-14.

798 (89) Lu, X.; Gu, W.; Zhao, L.; Ul Haque, M. F.; DiSpirito, A. A.; Semrau, J. D.; Gu, B.
799   Methylmercury Uptake and Degradation by Methanotrophs. *Sci. Adv.* **2017**, *3* (5), 1–6.
800   https://doi.org/10.1126/sciadv.1700041.

801 (90) Zhao, L.; Chen, H.; Lu, X.; Lin, H.; Christensen, G. A.; Pierce, E. M.; Gu, B. Contrasting
802   Effects of Dissolved Organic Matter on Mercury Methylation by Geobacter
803   Sulfurreducens PCA and Desulfovibrio Desulfuricans ND132. *Environ. Sci. Technol.*
804   **2017**, No. 51, 10468–10475. https://doi.org/10.1021/acs.est.7b02518.

805 (91) Liem-Nguyen, V.; Skyllberg, U.; Bjron, E. Thermodynamic Modeling of the Solubility
806   and Chemical Speciation of Mercury and Methylmercury Driven by Organic Thiols and
807   Micromolar Sulfide Concentrations in Boreal Wetland Soils. *Environ. Sci. Technol.* **2017**,
808   *51*, 3678–3686. https://doi.org/10.1021/acs.est.6b04622.

809 (92) Skyllberg, U.; Bloom, P. R.; Qian, J.; Lin, C. M.; Bleam, W. F. Complexation of
810   Mercury(II) in Soil Organic Matter: EXAFS Evidence for Linear Two-Coordination with
811   Reduced Sulfur Groups. *Environ. Sci. Technol.* **2006**, *40* (13), 4174–4180.
812   https://doi.org/10.1021/es0600577.

813 (93) Yoon, S. J.; Diener, L. M.; Boom, P. R.; Nater, E. A. N.; Bleam, W. F. B. X-Ray
814   Absorption Studies of CH3Hg+ -Binding Sites in Humic Substances. *Geochim.*
815   *Cosmochim. Acta* **2005**, *69* (5), 1111–1121. https://doi.org/10.1016/j.gca.2004.07.036.

816 (94) Liu, Y.-R.; Lu, X.; Zhao, L.; An, J.; He, J.-Z.; Pierce, E. M.; Johs, A.; Gu, B. Effects of
817   Cellular Sorption on Mercury Bioavailability and Methylmercury Production by
818   Desulfovibrio Desulfuricans ND132. *Environ. Sci. Technol.* **2016**, No. 50, 13335–13341.
819   https://doi.org/10.1021/acs.est.6b04041.

820 (95) Graham, A. M.; Bullock, A. L.; Maizel, A. C.; Elias, D. A.; Gilmour, C. C. Detailed
821   Assessment of the Kinetics of Hg-Cell Association, Hg Methylation, and Methylmercury

32

Degradation in Several Desulfovibrio Species. *Appl. Environ. Microbiol.* **2012**, *78* (20), 7337–7346. https://doi.org/10.1128/AEM.01792-12.

(96)   Schaefer, J. K.; Rocks, S. S.; Zheng, W.; Liang, L.; Gu, B.; Morel, F. M. M. Active Transport, Substrate Specificity, and Methylation of Hg(II) in Anaerobic Bacteria. *PNAS* **2011**, *108* (21), 8714–8719. https://doi.org/10.1073/pnas.1105781108.

(97)   Lin, H.; Lu, X.; Liang, L.; Gu, B. Cysteine Inhibits Mercury Methylation by Geobacter Sulfurreducens PCA Mutant ΔomcBESTZ. *Environ. Sci. Technol. Lett.* **2015**, *2*, 144–148. https://doi.org/10.1021/acs.estlett.5b00068.

(98)   Liem-Nguyen, V.; Skyllberg, U.; Björn, E. Methylmercury Formation in Boreal Wetlands in Relation to Chemical Speciation of Mercury(II) and Concentration of Low Molecular Mass Thiols. *Sci. Total Environ.* **2021**, *755* (142666), 1–9. https://doi.org/10.1016/j.scitotenv.2020.142666.

(99)   Sebestyen, S. D.; Verry, E. S.; Elling, A. E.; Kyllander, R. L.; Roman, D. T.; Burdick, J. M.; Lany, N. K.; Kolka, R. K. *Marcell Experimental Forest Peatland and Upland Water Table Elevations*, 2nd ed.; Forest Service Research Data Archive: Fort Collins, CO, USA, 2021. https://doi.org/https://doi.org/10.2737/RDS-2018-0002-2.

(100) Jonsson, S.; Skyllberg, U.; Nilsson, M. B.; Westlund, P. O.; Shchukarev, A.; Lundberg, E.; Björn, E. Mercury Methylation Rates for Geochemically Relevant Hg(II) Species in Sediments. *Environ. Sci. Technol.* **2012**, *46* (21), 11653–11659. https://doi.org/10.1021/es3015327.

(101) Hammerschmidt, C. R.; Fitzgerald, W. F. Geochemical Controls on the Production and Distribution of Methylmercury in Near-Shore Marine Sediments. *Environ. Sci. Technol.* **2004**, *38* (5), 1487–1495. https://doi.org/10.1021/es034528q.

(102) Lie, T. J.; Pitta, T.; Leadbetter, E. R.; Godchaux, W.; Leadbetter, J. R. Sulfonates: Novel Electron Acceptors in Anaerobic Respiration. *Arch. Microbiol.* **1996**, *166* (3), 204–210. https://doi.org/10.1007/s002030050376.

(103) Lie, T. J.; Leadbetter, J. R.; Leadbetter, E. R. Metabolism of Sulfonic Acids and Other Organosulfur Compounds by Sulfate-Reducing Bacteria. *Geomicrobiol. J.* **1998**, *15* (2), 135–149. https://doi.org/10.1080/01490459809378070.

(104) Visscher, P. T.; Gritzer, R. F.; Leadbetter, E. R. Low-Molecular-Weight Sulfonates, a Major Substrate for Sulfate Reducers in Marine Microbial Mats. *Appl. Environ. Microbiol.* **1999**, *65* (8), 3272–3278. https://doi.org/10.1128/aem.65.8.3272-3278.1999.

(105) Solomon, D.; Lehmann, J.; Zarruk, K. K. De; Dathe, J.; Kinyangi, J.; Liang, B.; Machado, S. Speciation and Long- and Short-Term Molecular-Level Dynamics of Soil Organic Sulfur Studied by X-Ray Absorption Near-Edge Structure Spectroscopy. **2011**. https://doi.org/10.2134/jeq2010.0061.

(106) Zhao, F. J.; Lehmann, J.; Solomon, D.; Fox, M. A.; McGrath, S. P. Sulphur Speciation and Turnover in Soils: Evidence from Sulphur K-Edge XANES Spectroscopy and Isotope Dilution Studies. *Soil Biol. Biochem.* **2006**, *38*, 1000–1007. https://doi.org/10.1016/j.soilbio.2005.08.013.

(107) Solomon, D.; Lehmann, J.; Kinyangi, J.; Pell, A.; Theis, J.; Riha, S.; Ngoze, S.; Amelung, W.; Du Preez, Ch.; Machado, S.; Ellert, B.; Janzen, H. Anthropogenic and Climate Influences on Biogeochemical Dynamics and Molecular-Level Speciation of Soil Sulfur. *Ecol. Appl.* **2009**, *19* (4), 989–1002.

(108) Churka Blum, S.; Lehmann, J.; Solomon, D.; Fávero, E.; Reynaldo, L.; Alleoni, F. Sulfur Forms in Organic Substrates Affecting S Mineralization in Soil. *Geoderma* **2013**, *200–*

868   *201*, 156–164. https://doi.org/10.1016/j.geoderma.2013.02.003.

869   (109)   Friedrich, C. G.; Rother, D.; Bardischewsky, F.; Quentmeier, A. Oxidation of Reduced
870   Inorganic Sulfur Compounds by Bacteria: Emergence of a Common Mechanism? *Appl.*
871   *Environ. Microbiol.* **2001**, *67* (7), 2873–2882. https://doi.org/10.1128/AEM.67.7.2873.

872   (110)   Luther, G. W.; Findlay, A. J.; Macdonald, D. J.; Owings, S. M.; Hanson, T. E.; Beinart, R.
873   A.; Girguis, P. R. Thermodynamics and Kinetics of Sulfide Oxidation by Oxygen: A Look
874   at Inorganically Controlled Reactions and Biologically Mediated Processes in the
875   Environment. *Front. Microbiol.* **2011**, *2*, 1–9. https://doi.org/10.3389/fmicb.2011.00062.

876   (111)   Feng, S.; Ai, Z.; Zheng, S.; Gu, B. Effects of Dryout and Inflow Water Quality on
877   Mercury Methylation in a Constructed Wetland. *Water Air Soil Pollut.* **2014**, *225* (1929),
878   1–11. https://doi.org/10.1007/s11270-014-1929-6.

879   (112)   Munthe, J.; Bodaly, R. A. D.; Branfireun, B. A.; Driscoll, C. T.; Gilmour, C. C. Recovery
880   of Mercury-Contaminated Fisheries. *J. Hum. Environ.* **2007**, *36* (1), 33–44.

881